

Simultaneous first and second order percolation transitions in interdependent networks

Dong Zhou,¹ Amir Bashan,¹ Reuven Cohen,² Yehiel Berezin,¹ Nadav Shnerb,¹ and Shlomo Havlin¹

¹*Department of Physics, Bar-Ilan University, Ramat Gan 52900, Israel*

²*Department of Mathematics, Bar-Ilan University, Ramat Gan 52900, Israel*

(Dated: October 30, 2018)

In a system of interdependent networks, an initial failure of nodes invokes a cascade of iterative failures that may lead to a total collapse of the whole system in a form of an abrupt first order transition. When the fraction of initial failed nodes $1 - p$ reaches criticality, $p = p_c$, the abrupt collapse occurs by spontaneous cascading failures. At this stage, the giant component decreases slowly in a plateau form and the number of iterations in the cascade, τ , diverges. The origin of this plateau and its increasing with the size of the system remained unclear. Here we find that simultaneously with the abrupt first order transition a spontaneous second order percolation occurs during the cascade of iterative failures. This sheds light on the origin of the plateau and on how its length scales with the size of the system. Understanding the critical nature of the dynamical process of cascading failures may be useful for designing strategies for preventing and mitigating catastrophic collapses.

I. INTRODUCTION

Interdependent network systems attract a growing interest in the last years [1–21]. They represent real world systems composed of different types of interrelations, connectivity links between entities (nodes) of the same network to share supply or information and dependency links which represent a dependency of one node on the function of another node in another network. Consequently, failure of nodes may lead to two different effects: removal of other nodes from the same network which become disconnected from the giant component and failure of dependent nodes in other networks. The synergy between these two effects leads to an iterative chain cascading of failures. Buldyrev *et al* [5] show that, in a system of two fully interdependent random networks, when the fraction of failed nodes $1 - p$ is smaller than a critical value, $p > p_c$, the cascading failures stop after some iterations and a finite fraction of the system, $P_\infty > 0$, remains functioning and connected to the giant component. A larger initial damage, $p < p_c$, invokes a cascading failure that fragments the entire system and $P_\infty = 0$. Thus, when p approaches p_c from above, the giant component, P_∞ , discontinuously jumps to zero in a form of a first order transition. The number of iterations in the cascade, τ , diverges when p approaches p_c , a behavior that was suggested as a clear indication for the transition point in numerical simulations [22].

Among the main features found are the collapse of the system with time (steps of cascading failures) in a plateau form (see Fig. 1), and the increase of the plateau length with the system size. Although this phenomena was observed in different models and in real data, its origin remained unclear [5]. To understand the origin of this phenomena we focus on fully interdependent Erdős-Rényi (ER) networks. Surprisingly, we find here that during the abrupt collapse there appears a hidden spontaneous second order percolation transition that controls the cascading failures, as demonstrated in Fig. 1. We show here that this simultaneous second order phase transition, characterized by long branching trees near criticality, is the origin of the observed long plateau regime in the cascading failures and its dependence on system size. Moreover, the second order transition sheds light on the critical behavior ob-

served in the collapse of real world systems such as the power law distribution of blackout sizes [23–26].

We also find, as a result of this new understanding, that even though the mean-field (MF) approximations are found to be accurate in predicting p_c and P_∞ , it does not represent the dynamical process of cascading failures near criticality. This is since, the critical dynamics is strongly affected by random fluctuations due to the second order transition which are not considered in the MF approach. We study the effect of these fluctuations on the total number of iterations τ at criticality and find that its average and standard deviation scale as $N^{1/3}$, in contrast to the MF prediction of $\langle \tau \rangle \sim N^{1/4}$ [5]. We present a theory for the dynamics at criticality, which explains the origin of this difference.

II. MODEL OF INTERDEPENDENT NETWORKS

In the fully interdependent networks model, A and B are two networks of the same size N . Each A -node a_i depends on exactly one randomly-chosen B -node b_j , and b_j also only depends on a_i . The initial attack is removing randomly a fraction $1 - p$ of A -nodes in one network. Nodes in one network that depend on removed nodes in the other network are also removed, causing a cascade of failures. As nodes and edges are removed, each network breaks up into connected components (clusters). It is known that for single random networks, there is at most one component (giant component) which occupies a finite fraction of all N nodes (see [27]). We assume that only nodes belonging to the giant component connecting a finite fraction of the network are still functional. Since the two networks have different topological structures, the failure will spread as a cascading process in the system [18, 28, 29]. Here, one time step means that dependency failures and percolation failures occur at a given iteration in networks A and B respectively, and each network reaches a new smaller giant component.

The MF theory of this model with ER networks with average degrees k_A and k_B has been developed using generating functions of the degree distribution. This theory predicts the giant component size as a function of p , and accurately

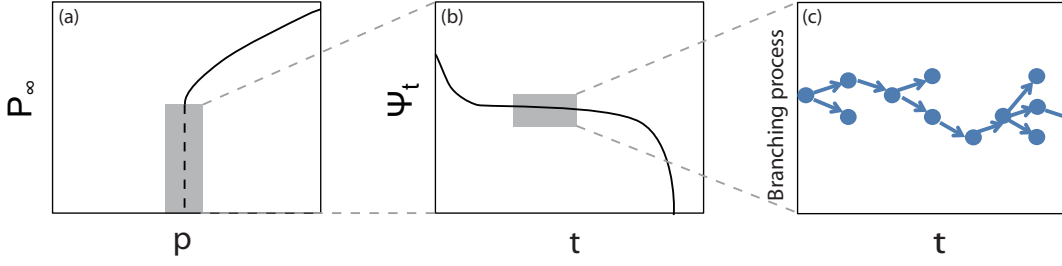


FIG. 1. Demonstration of the simultaneous first and second order transitions in cascading failures of interdependent networks. At the critical point p_c , (a) the mutual giant component has a sudden jump to zero, while (b) the dynamical process of cascading failures is governed by a long plateau stage. In this plateau stage, a second order percolation occurs, which is (c) characterized by a random branching process at criticality, i.e., average branching factor is one (see Fig. 3(b)).

evaluate the first order phase transition threshold p_c^{MF} for the infinite-size system. In fact, each realization in the simulation has its own critical threshold which we denote by p_c . In this paper, a new realization means that we generate networks A and B again, as well as the interdependency links, and then we perform the initial attack according to a new random attack order (see [30]). Note that for $N \rightarrow \infty$, p_c values in single realizations are the same and equal to p_c^{MF} .

III. SCALING BEHAVIOR IN THE CRITICAL DYNAMICS

Here, we investigate the dynamics of the critical cascading failures for each single realization of a pair of finite coupled networks. For simplicity, networks A and B have the same average degree k . The value of p_c of each realization, can be determined accurately by randomly removing nodes one by one until the system fully collapses.

Fig. 2(a) exhibits several realizations of simulations at p_c^{MF} . As seen at criticality, the total time τ has large fluctuations. Each realization has a stage of time steps (a plateau) where the giant component of network A decreases very slowly. Before or after this plateau stage, the cascading failure process is much faster.

Fig. 2(b) and Fig. 2(c) show the scaling behaviors of the mean and the standard deviation of τ as a function of N and $p - p_c$. In our simulations, we consider $p \leq p_c$, and only those realizations that fully collapse. We wish to understand how N and $p - p_c$ affect the mean and the standard deviation of the total time τ .

It can be seen from Fig. 2(b) that $\langle \tau \rangle$ increases with N as $\langle \tau \rangle \sim N^{1/3}$ at $p = p_c$. However, when $p < p_c$, $\langle \tau \rangle$ becomes constant for large values of N . Thus, we assume the following scaling function,

$$\langle \tau \rangle \sim N^{1/3} \cdot f(u), \quad (1)$$

where $u = (p_c - p) \cdot N^{1/\alpha}$, and $f(u)$ is a function which satisfies: $f(u) \sim \text{const.}$ for $u \ll 1$, $f(u) \sim u^{-\alpha/3}$ for $u \gg 1$, and we determine α such that the best scaling occurs.

To test Eq. (1) and identify α , we plot in Fig. 2(c) $\langle \tau \rangle / N^{1/3}$ versus u . We find that the best choice of α for obtaining a

good scaling collapse is $\alpha = 3/2$. In this way, we can see that the slope of each curve changes from 0 to about $-1/2$ at $u = (p_c - p) \cdot N^{2/3} \approx 1$. Therefore, the scaling behavior of $\langle \tau \rangle$ for $N < N^* \sim (p_c - p)^{-3/2}$ is

$$\langle \tau \rangle \sim N^{1/3}, \quad (2)$$

independent of p (Fig. 2(b)). This means that system sizes of $N < N^*$ are at criticality even though $p < p_c$. For $N > N^*$, $\langle \tau \rangle \sim N^{1/3} \cdot u^{-1/2} = (p_c - p)^{-1/2}$, independent of N (Fig. 2(b)) (non-critical behaviors). This yields the crossover $N^* \sim (p_c - p)^{-\alpha} = (p_c - p)^{-3/2}$, between the critical behavior for $N < N^*$ and non-critical for $N > N^*$. For $p \rightarrow p_c$, $N^* \rightarrow \infty$ and for all N one observes the critical behavior. The crossover system size, N^* , can be regarded as a correlation size analogously to the correlation length in regular percolation [31, 32].

Fig. 2(b) also illustrates the scaling behaviors of the standard deviation, $\text{std}(\tau)$. For $p = p_c$, we obtain $\text{std}(\tau) \sim N^{1/3}$, i.e., it increases as the same rate as the mean. However, for $p < p_c$, the slope in the right tail of $\text{std}(\tau)$ in Fig. 2(b) is about $-1/3$. Thus, we assume a scaling function for $\text{std}(\tau)$:

$$\text{std}(\tau) \sim N^{1/3} \cdot g(u), \quad (3)$$

where $u = (p_c - p) \cdot N^{1/\alpha}$, and $g(u)$ satisfies: $g(u) \sim \text{const.}$ for $u \ll 1$, and $g(u) \sim u^{-2\alpha/3} = u^{-1}$ for $u \gg 1$.

Fig. 2(c) shows that the scaling behavior of $\text{std}(\tau)$ assumed in Eq. (3) is supported by simulations with the best choice $\alpha = 3/2$ as for $\langle \tau \rangle$. The slope of the right tail in Fig. 2(c) is indeed -1 . Thus, for $N < N^*$, we have the critical behavior: $\text{std}(\tau) \sim N^{1/3}$; and for $N > N^*$, $\text{std}(\tau) \sim N^{1/3} \cdot u^{-1} = N^{-1/3} (p_c - p)^{-1}$. Thus, we have the non-critical behavior also consistent with Fig. 2(b).

IV. THE SPONTANEOUS SECOND ORDER PERCOLATION TRANSITION

Next we explore the mechanism behind the scaling behaviors near p_c . We show that it is due to a spontaneous second order percolation transition and explain the deviation from the MF theory. The failure size, s_t , the number of A -nodes that

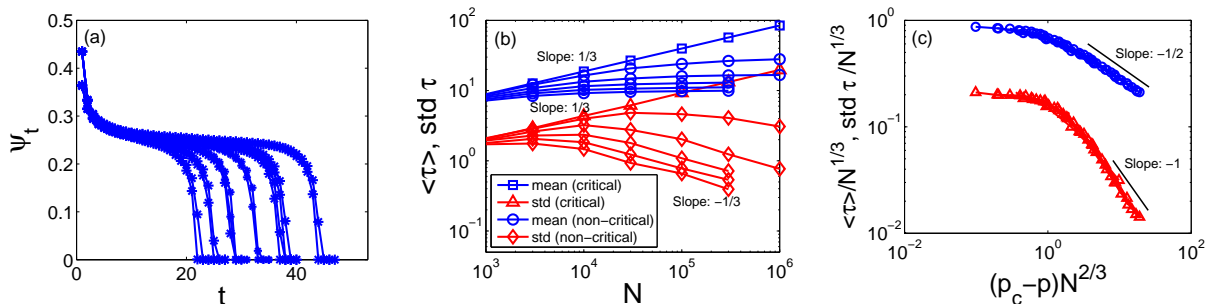


FIG. 2. (Color online) **a.** Dynamical process of the giant component size ψ_t of network A in simulation at p_c^{MF} (15 realizations). **b.** Scaling behavior of the mean (blue) and the standard deviation (red) of the total time τ at p_c (critical) or below p_c (non-critical) for each realization. Each curve here corresponds to a fixed value of p . **c.** The scaled version of (b). We consider for Fig. 2(a) the case $N = 300\,000$ and $k = 5$ with 15 realizations. For Figs. 2(b) and 2(c), we have $k = 5$ for the different N values we analyzed. Each point here is the mean or the standard deviation over 200 realizations of $N = 10^6$, and order of 10^4 realizations for $N \leq 300\,000$.

fail at time step t , during the plateau from the coupled networks system, is a zero fraction of the network size N . This is supported by simulations shown in Fig. 4(a). We regard each node that fails due to dependency at the beginning of the plateau stage as a root, a_i , of a failure tree (see Fig. 1). After that, the removal of each root a_i will cause the failure of several other A -nodes due to percolation. Then, several B -nodes will fail due to dependency and percolation in network B . At the next time step, several A -nodes further fail due to dependency and percolation, which can be regarded as the result of the original removal of the root node a_i . Notice that the failures in network A caused by removing different single nodes a_i have very few overlaps due to the randomness and the large size of N . Therefore, we can describe the plateau stage by the growth of all these independent failure trees with the branching factor $\eta_t = s_{t+1}/s_t$.

Fig. 3(a) and Fig. 3(b) show the variation of s_t and η_t respectively in a typical realization that finally reached a total collapse. We observe that η_t increases during the cascades from below 1 to around 1 (with some fluctuations) at the plateau, and finally to above 1 when the system starts to collapse. The value of η_t is smaller than 1 in the beginning of the cascading process since the individual networks are still well connected and a large damage in one network leads to a smaller damage in the second network (see Fig. 3(a)). As cascading progresses the value of η_t increases since both networks become more dilute and a failure in one step leads to relatively higher damage in the next step (see Fig. 3(b)). In this process the spontaneous behavior of η_t generates a new phase transition. When η_t approaches 1 the system *spontaneously enters* a second order percolation transition where the cascading trees become critical branching processes ([31]) of typical length of $N^{1/3}$ as explained below. These long trees are the origin of the long plateau observed in Fig. 2(a).

The plateau stage starts when each of the n failed nodes at iteration T_1 leads, in average (we refer to the fluctuations explicitly in the following), to failure of another single node (see [33]). This is a stable state, leading to the divergence of τ for $N \rightarrow \infty$. In a finite system of size N , however, the accumulated failures slightly reduce p and the number of failures at

each iteration gradually increases. This bias can be estimated by considering the percolation on single networks as follow.

At each time step t , the giant component size ψ_t of network A can be equivalently regarded as randomly attacking a fraction $1 - p$ on a single ER network. This specific value of p , called the effective p and denoted here by p_{eff} , can be obtained theoretically by solving the equation $\psi_t = p \cdot g(p)$, where $g(p)$ is the fraction of nodes in the giant component after randomly removing a fraction p of nodes (see [5]).

Moreover, η_t can be related to the branching factor for a single network. Consider randomly removing a fraction $1 - p$ of nodes in an ER network, which makes some other nodes non-functional due to percolation, i.e., being disconnected from the giant component. Then, we randomly remove one more node within the giant component, and we use η_{single} to denote the number of nodes that fail additionally due to percolation. Notice that η_{single} is the branching factor for the additionally-removed node. Fig. 3(c) shows the relation between p and η_{single} for an ER network. Note that the branching factor diverges (for infinite systems) when $p \rightarrow p_c^+$, and converges to 0 when $p \rightarrow 1$. Let \tilde{p} be the critical value of p where $\langle \eta_{single} \rangle = 1$. Then we see from Fig. 3(c) that $\tilde{p} \approx 0.35$.

For two coupled ER networks, at each time step t in the plateau stage, the difference between the giant components of networks A and B is small compared to the giant component sizes. Thus, each $A(B)$ -node that fails due to dependency can be approximately regarded as randomly removing one more node from the giant component of network A (B). Therefore, $\eta_t \approx \langle \eta_{single} \rangle^2$ for the plateau stage. Notice that when $\langle \eta_{single} \rangle = 1$, η_t also equals to 1, and the threshold $\tilde{p} \approx 0.35$ is also valid for coupled ER networks. This can be seen in Fig. 3(d), which shows the evolution of p_{eff} in the same realization of Fig. 3. We can see that the interaction between p_{eff} and $\langle \eta_t \rangle$ is a determinate factor for the plateau stage. As shown in Fig. 3, when p_{eff} gets smaller, η_t increases to about 1. This causes a range of time steps where s_t is approximately a constant with some random fluctuations. Here, the random fluctuations of η_t will determine the end of the cascading process, with or without a total collapse.

Based on these observations, we assume a random process

of cascading failures starting at the beginning of the plateau state at $t = T_1$. Let $n = s_{T_1}$, which is also the number of independent failure trees, and consider time steps $T = t - T_1$. The variation of the failure sizes s_T are determined by both the systematic bias and the random fluctuations. Here, the random fluctuations can be described by a Gaussian random walk from the value of n .

Assuming that $p_{eff} = \tilde{p}$, and $\eta_T = 1$ at $T = 0$, and η_T decreases linearly when p_{eff} increases near \tilde{p} : $\eta_T = 1 - C \cdot \Delta p_{eff}$. Here, C is a positive constant, and Δp_{eff} is the increment of p_{eff} from \tilde{p} , which is approximately the variation of the giant component size of network A . Therefore, $\Delta p_{eff} = -\frac{\sum_{i=0}^T s_i}{N}$. At $T = 1$, we have $s_1 = n \cdot (1 - C \Delta p_{eff}) = n \cdot (1 + C \frac{n}{N}) = n + \frac{C}{N} n^2$. At $T = 2$, we have $s_2 = s_1 \cdot (1 + \frac{C}{N}(n + s_1))$. After casting down small terms, we obtain $s_2 = n + 3 \frac{C}{N} n^2$. Similarly, we can obtain at T :

$$s_T = n + \left(\sum_{i=1}^T i \right) \cdot \frac{C}{N} n^2 = n + \frac{T(T+1)}{2} \cdot \frac{C}{N} n^2. \quad (4)$$

Therefore, the order of the systematic bias of failure sizes from T_1 to T_2 is $\frac{n^2 T^2}{N}$. If at some iteration the number of failures becomes zero the cascading process stops and the system survives. This can happen when $n - \sqrt{n} \sqrt{T} = 0$, thus,

$$T_{stop} \sim \sqrt{n}. \quad (5)$$

If it does not stop, the cascading failures continue, and for large T the bias will grow (faster than the fluctuations) leading to complete collapse. The balance between the bias and the fluctuations may continue as long as

$$\frac{n^2 T^2}{N} \sim \sqrt{n} \sqrt{T}. \quad (6)$$

Equations (5) and (6) yield that $n \sim T \sim N^{1/3}$, which is supported by our simulation results in Fig. 2(b) showing $\langle \tau \rangle \equiv T \sim N^{1/3}$.

The above analysis also leads to the scaling law for the failure size at the beginning of the plateau stage: $n \sim N^{1/3}$. This is supported by simulations shown in Fig. 4(a), which exhibits the average failure size $\langle s_T \rangle$ along the plateau stage near criticality.

The critical behavior at the plateau is also represented in the distribution of failure tree sizes obtained in simulations shown in Fig. 4(b). Here, we determine the beginning and the end of the plateau (see [33]), and identify all A -nodes that fail due to dependency in each of the parallel failure trees. At each time step, the growth of each tree is determined by the branching factor η_t . On the plateau, most trees will rapidly die out, while several trees keep growing and become large. Fig. 4(b) displays the PDF of the tree size S_{tree} , which is the total number of nodes on a failure tree from the root to the time step where it terminates. We can see that the total tree size has a power-law distribution with a slope of approximately $-3/2$. It

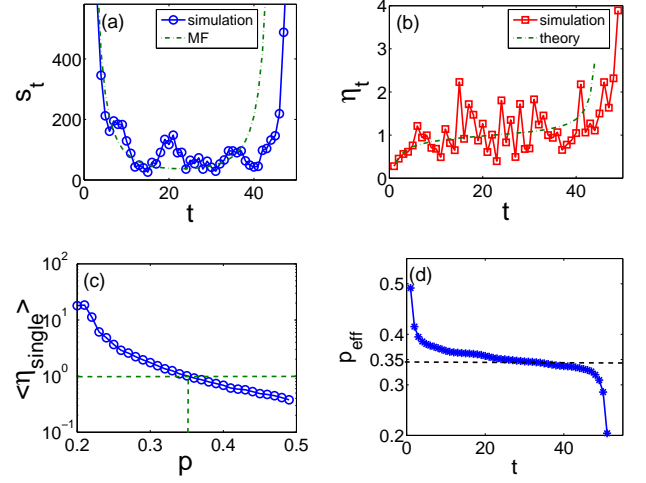


FIG. 3. (Color online) **a.** The (blue) line with circles is the variation of failure sizes s_t (only the plateau stage) for one realization in simulation. Here, $k = 5$, $p = p_c^{MF}$ and $N = 50\,000$. The (green) dashed dotted line shows s_t for the MF case for $k = 5$, $N = 50\,000$, and $p = 2.454/k$ slightly below $p_c^{MF} = 2.4554/k$. **b.** The (red) line with rectangles shows the variation of the average branching factor η_t for one realization in simulation. Here, $k = 5$, $p = p_c^{MF}$ and $N = 50\,000$. The (green) dashed dotted line shows η_t of the analytic MF solution. Here, $k = 5$, $N = 50\,000$ and $p = 2.4536/k$ below p_c^{MF} . In both (a) and (b), the MF values have similar behaviors as the simulation values, but the MF curves are smooth and show no fluctuations. **c.** The average branching factor $\langle \eta_{single} \rangle$ for different values of p on a single ER network. Here, $k = 5$, $N = 250\,000$ for 3000 realizations. A threshold \tilde{p} where $\langle \eta_{single} \rangle = 1$ can be observed at $p = \tilde{p} \approx 0.35$. **d.** The variation of the effective p for one realization in the simulations. Here, $k = 5$, $p = p_c^{MF} = 2.4554/k$ and $N = 50\,000$.

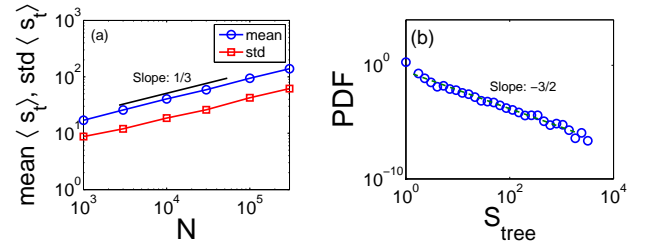


FIG. 4. (Color online) **a.** Scaling results of the mean and the standard deviation of the average failure size $\langle s_T \rangle$ from T_1 to T_2 , which is also the approximate number of branching processes for $p = p_c$ and $k = 5$. Number of realizations is same as in Fig. 2(b). **b.** PDF of failure tree sizes S_{tree} for the case $p = p_c$, $k = 3$, $N = 100\,000$ and 4537 trees in 80 realizations.

is interesting to note that such a distribution is associated with cluster size distributions in second order percolation transitions, see e.g., [27, 31, 32] and obtained in classical models of self-organized criticality [34–38]. Notice also that the same critical exponent has been observed in real data [23–26].

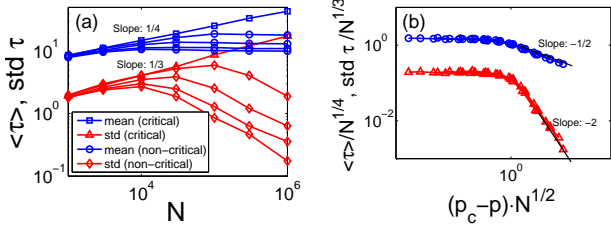


FIG. 5. (Color online) **a**. Scaling behaviors of the mean (blue) and the standard deviation (red) of the total time τ at $p_c^{MF} = 2.4554/k$ (critical) or below p_c^{MF} (non-critical). Here, we consider $k = 5$, and the number of realizations is $M = 3000$. **b**. Scaled version of (a). Two more values of p are included: $p = 0.4908$ and $p = 0.491$.

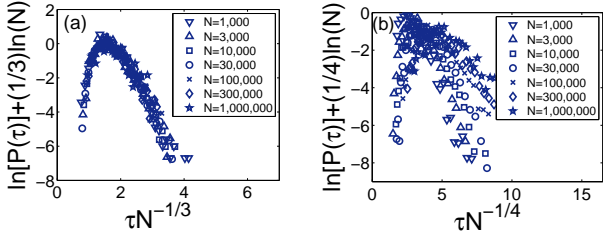


FIG. 6. (Color online) **a**. Scaled PDF of τ using the exponent $1/3$ at $p = p_c$ for single realizations. Here, $k = 5$, and the number of realizations is the same as in Fig. 2(b). **b**. Scaled PDF of τ using the exponent $1/4$.

V. RELATION BETWEEN THE CRITICAL SCALING AND THE MEAN-FIELD CASE

Buldyrev *et al.* [5] found both analytically and numerically the scaling behavior $\langle \tau \rangle \sim N^{1/4}$ at p_c^{MF} , which is significantly different from the critical scaling result $N^{1/3}$ found here at p_c of each realization. Fig. 5 shows the scaling behaviors of both $\langle \tau \rangle$ and $\text{std}(\tau)$ at and below p_c^{MF} . As can be seen, the mean behavior is indeed consistent with the MF predictions of [5]. We will explain in this section this seemingly discrepancy by analyzing the theoretical relationship between the scaling behaviors at p_c of single realizations and at the MF prediction p_c^{MF} .

In Fig. 5, we observe the scaling rule of $\langle \tau \rangle$: $\langle \tau \rangle \sim N^{1/4} \cdot f(u)$, where, $u = (p_c^{MF} - p) \cdot N^{1/\alpha}$, and $\alpha = 2$. Then, we have $f(u) \sim 1$ for $u \ll 1$, and $f(u) \sim u^{-1/2}$ for $u \gg 1$. Finally, for $N < N^* \sim (p_c - p)^{-3/2}$, $\langle \tau \rangle \sim N^{1/4}$, and for $N > N^*$, $\langle \tau \rangle \sim (p_c - p)^{-1/2}$. Compared with the scaling results for single realizations, Eqs. (1) and (2), the main difference is the exponent $1/4$ of the scaling of $\langle \tau \rangle$ with N . To further validate our new scaling law, $\langle \tau \rangle \sim N^{1/3}$ at $p = p_c$ of single realizations, we also compare in Fig. 6 the two scaling laws for the PDF of τ : Fig. 6(a) presents the PDF of τ for different values of N according to the scaling assumption $\tau \sim N^{1/3}$, whereas Fig. 6(b) gives the PDF of τ according to the scaling assumption $\tau \sim N^{1/4}$. As can be seen from these figures, the assumption $\tau \sim N^{1/3}$ seems to better fit the scaling for single realizations, further supporting Eq. (2).

The origin of the MF observation, $\langle \tau \rangle \sim N^{1/4}$ and $\text{std}(\tau) \sim N^{1/3}$ (see Fig. 5), which deviates from Eq. (2) for single realizations, can be explained by considering the fluctuations which do not appear in the MF case.

Given $\langle \tau \rangle \sim N^{1/3}$ at p_c , and $\langle \tau \rangle \sim (p_c - p)^{-1/2}$ when p is below p_c , the scaling behavior at p_c^{MF} can be regarded as the expectation of $\langle \tau \rangle$ below p_c :

$$\langle \tau \rangle_{MF} = \int_0^\infty \langle \tau \rangle \cdot D(x) dx, \quad (7)$$

where $x = p_c - p$, and $D(x)$ is its probability density. From the scaling results in Fig. 2(c), we know that $\langle \tau \rangle \sim N^{1/3}$, for $p_c - p < N^{-2/3}$ and $\langle \tau \rangle \sim (p_c - p)^{-1/2}$, for $p_c - p > N^{-2/3}$. We also assume that the value of p_c follows a Gaussian distribution $N(p_c^{MF}, \sigma^2)$ (This is supported by the distribution of p_c in simulations, see Fig. 7 in the Appendix.) above p_c^{MF} , where $\sigma \sim N^{-1/2}$. Therefore,

$$\begin{aligned} \langle \tau \rangle_{MF} = I_1 + I_2 \sim & \int_0^{N^{-2/3}} N^{1/3} \cdot \frac{1}{\sqrt{2\pi}\sigma} \exp\left(-\frac{x^2}{2\sigma^2}\right) dx \\ & + \int_{N^{-2/3}}^\infty x^{-1/2} \cdot \frac{1}{\sqrt{2\pi}\sigma} \exp\left(-\frac{x^2}{2\sigma^2}\right) dx. \end{aligned} \quad (8)$$

Let $y = x \cdot \sqrt{N}$, which finally yields $I_1 \sim N^{1/6}$ and $I_2 \sim N^{1/4}$, from which follows $\langle \tau \rangle_{MF} = I_1 + I_2 \sim N^{1/4}$ for large N .

Similarly, we can also calculate the variance of τ using $\text{var}(\tau) = \langle \tau^2 \rangle - \langle \tau \rangle^2$, and then estimate the scaling result for the standard deviation at p_c^{MF} . We can finally obtain $\text{std}(\tau) \sim N^{1/4}$, instead of $N^{1/3}$, seen in Fig. 5(a). The explanation of this deviation can be understood by performing accurate numerical integrals for the analogous Eq. (8) for the standard deviation. This accurate integration shows that for small values of N , the scaling of $\text{std}(\tau)$ with N can be approximated as $\text{std}(\tau) \sim N^{1/3}$. However, for large N , the slope decreases to $N^{1/4}$. This might explain for the slope $1/3$ of $\text{std}(\tau)$ at p_c^{MF} observed in simulations, as shown in Fig. 5(a).

VI. SUMMARY

In this paper, we identified a spontaneous second order percolation transition occurring during the cascading failures which controls the first order abrupt transition. This spontaneous transition is characterized by cascading of failure trees whose size distribution is power law with an exponent $-3/2$ during the plateau stage. This explains the origin of the long plateau and its scaling with N found in cascading process near the abrupt collapse of the coupled networks system. We also uncovered the theoretical relationship between the two seemingly contradictory scaling, $\langle \tau \rangle \sim N^{1/4}$ at the mean-field criticality and $\langle \tau \rangle \sim N^{1/3}$ at p_c of single realizations, by considering the deviation of p_c in different realizations.

ACKNOWLEDGMENTS

We thank DTRA, ONR, BSF, the LINC (No. 289447) and the Multiplex (No. 317532) EU projects, the DFG, and the

Israel Science Foundation for support. We thank Michael M. Danziger for helpful discussions.

-
- [1] J. Laprie, K. Kanoun, and M. Kaniche, *Lect. Notes Comput. Sci.* **4680**, 54 (2007).
- [2] V. Rosato, L. Issacharoff, F. Tiriticco, S. Meloni, S. De Porcellinis, and R. Setola, *Int. J. Crit. Infrastruct.* **4**, 63 (2008).
- [3] S. Panzieri and R. Setola, *Int. J. Model. Ident. Contr.* **3**, 69 (2008).
- [4] A. Vespignani, *Nature (London)* **464**, 984 (2010).
- [5] S. V. Buldyrev, R. Parshani, G. Paul, H. E. Stanley, and S. Havlin, *Nature (London)* **464**, 1025 (2010).
- [6] R. Parshani, S. V. Buldyrev, and S. Havlin, *Phys. Rev. Lett.* **105**, 048701 (2010).
- [7] J. Gao, S. V. Buldyrev, H. E. Stanley, and S. Havlin, *Nature Physics* **8**, 40 (2011).
- [8] E. A. Leicht and R. M. D'Souza, "Percolation on interacting networks," (2009), arXiv:0907.0894.
- [9] R. G. Morris and M. Barthelemy, *Phys. Rev. Lett.* **109**, 128703 (2012).
- [10] A. Saumell-Mendiola, M. A. Serrano, and M. Boguñá, *Phys. Rev. E* **86**, 026106 (2012).
- [11] J. Shao, S. V. Buldyrev, S. Havlin, and H. E. Stanley, *Phys. Rev. E* **83**, 036116 (2011).
- [12] J. Gao, S. V. Buldyrev, S. Havlin, and H. E. Stanley, *Phys. Rev. Lett.* **107**, 195701 (2011).
- [13] X. Huang, J. Gao, S. V. Buldyrev, S. Havlin, and H. E. Stanley, *Phys. Rev. E* **83**, 065101 (2011).
- [14] S. Gómez, A. Díaz-Guilera, J. Gómez-Gardeñes, C. J. Pérez-Vicente, Y. Moreno, and A. Arenas, *Phys. Rev. Lett.* **110**, 028701 (2013).
- [15] J. Aguirre, D. Papo, and J. M. Buldú, *Nature Physics* **9**, 230 (2013).
- [16] C. D. Brummitt and E. A. L. R. M. D'Souza, *Proc. Natl. Acad. Sci.* **109**, E680 (2012).
- [17] G. Bianconi, *Phys. Rev. E* **87**, 062806 (2013).
- [18] D. Cellai, E. López, J. Zhou, J. P. Gleeson, and G. Bianconi, *Phys. Rev. E* **88**, 052811 (2013).
- [19] F. Radicchi and A. Arenas, *Nature Physics* **9**, 717 (2013).
- [20] W. Li, A. Bashan, S. V. Buldyrev, H. E. Stanley, and S. Havlin, *Phys. Rev. Lett.* **108**, 228702 (2012).
- [21] A. Bashan, Y. Berezin, S. V. Buldyrev, and S. Havlin, *Nature Physics* **9**, 667 (2013).
- [22] R. Parshani, S. V. Buldyrev, and S. Havlin, *Proc. Natl. Acad. Sci.* **108**, 1007 (2011).
- [23] B. A. Carreras, D. E. Newman, I. Dobson, and A. B. Poole, *IEEE Trans. Circuits Syst., I: Fundam. Theory Appl.* **51**, 1733 (2004).
- [24] Å. J. Holmgren and S. Molin, *J. Infrastruct. Syst.* **12**, 243 (2006).
- [25] J. Bakke, A. Hansen, and J. Kertész, *Europhys. Lett.* **76**, 717 (2006).
- [26] G. Ancell, C. Edwards, and V. Krichtal, in *Electricity Engineers Association 2005 Conference: Implementing New Zealand's Energy Options* (Auckland, New Zealand, 2005).
- [27] R. Cohen and S. Havlin, *Complex Networks: Structure, Robustness and Function* (Cambridge University Press, 2010).
- [28] R. Parshani, C. Rozenblat, D. Ietri, C. Ducruet, and S. Havlin, *Europhys. Lett.* **92**, 68002 (2010).
- [29] Y. Hu, D. Zhou, R. Zhang, Z. Han, C. Rozenblat, and S. Havlin, *Phys. Rev. E* **88**, 052805 (2013).
- [30] We tested also by taking a few different realizations and keeping the network structures but changing only the attack order. The results have been found to be very similar, as seen in Fig. 8.
- [31] A. Bunde and S. Havlin, *Fractals and Disordered Systems* (Springer, 1996).
- [32] D. Stauffer and A. Aharony, *Introduction to Percolation Theory* (Taylor & Francis, 1992).
- [33] In order to estimate the length of the plateau stage, we introduce a method to define the beginning, T_1 , and the end, T_2 , of the plateau in each realization. In Fig. 3(a), we find the time step T_f of the first local minimum and T_l of the last local minimum. Then, we define a threshold $d = 2 \cdot \frac{1}{T_l - T_f + 1} \cdot \sum_{t=T_f}^{T_l} s_t$, which is twice the average failure size between these two minimums. This is because the s_t values always have some random fluctuations above or below the mean value, which should be the same order as the mean. Therefore, we use twice the mean as the threshold for including such fluctuations. Then, we define T_1 and T_2 as the first time step and the last one where $s_t \leq d$.
- [34] B. A. Carreras, V. E. Lynch, I. Dobson, and D. E. Newman, *Chaos* **14**, 643 (2004).
- [35] J. Chen, J. S. Thorp, and I. Dobson, *Int. J. Electr. Power Energy Syst.* **27**, 318 (2005).
- [36] D. P. Nedic, I. Dobson, D. S. Kirschen, B. A. Carreras, and V. E. Lynch, *Int. J. Electr. Power Energy Syst.* **28**, 627 (2006).
- [37] I. Dobson, B. A. Carreras, and D. E. Newman, *Probab. Eng. Inform. Sc.* **19**, 15 (2005).
- [38] I. Dobson, B. A. Carreras, and D. E. Newman, in *37th Hawaii International Conference on System Sciences* (Hawaii, 2004).

VII. APPENDIX

1. Distribution of p_c around the mean-field prediction.

Fig. 7 shows the PDF of the normalized values of p_c : $p'_c \equiv \frac{p_c - \langle p_c \rangle}{\text{std}(p_c)}$, compared with a standard Gaussian distribution. Here we can find that p_c follows a Gaussian distribution around the MF prediction p_c^{MF} . This supports our assumption in the main text that p_c follows a Gaussian distribution.

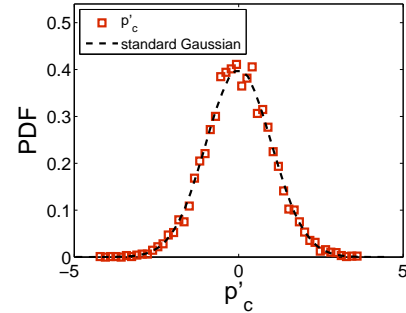


FIG. 7. (Color online) PDF of the normalized p_c , p'_c , for single realizations in simulations, compared with the standard Gaussian distribution. Here, $k = 5$, $N = 30\,000$ for 6000 realizations. We see here that the value of p_c follows quite well a Gaussian distribution.

2. Effect of the randomness in network structures

In our simulations, there are two types of randomness in each realization: the structure of ER network and the random initial attack. We always change both the networks and the attack order at the beginning of each realization. However, when the network is large enough, the randomness of the network structure is not needed for our results. In Fig. 8, we compare the scaling behaviors of the total number of cascade τ in two cases: varying both the networks and the attack order, and varying only the attack order for a given realization. We find that they have very similar behavior.

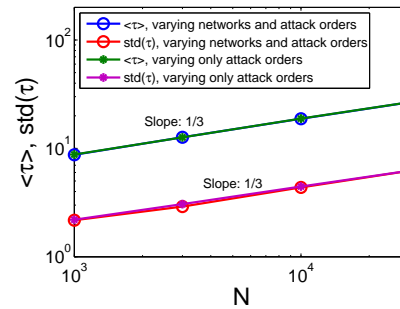


FIG. 8. (Color online) Scaling behaviors of the mean and the standard deviation of the total time τ at p_c for individual realizations. Two cases are compared here: in each realization, varying both the networks and the attack order, and only varying the attack order. We consider $k = 5$ with 3000 realizations for different N values.